

Responses to the editorial comments

1) The newly inserted Figure 10 with the kriging variance indicates extremely high numbers that are not comparable to the order of magnitude of the N₂O fluxes presented in Figure 9. Could you please double check these numbers or explain where these high values come from? Alternatively, you could present the standard deviation which would have the same unit as the fluxes in Figure 9.

Author's Response:

Yes, we agreed. After having a double check, we found that the formula for computing the kriging variance was incorrect. We are very sorry for having made such a careless mistake. Prior to the geostatistical analysis, our N₂O fluxes data were logit-transformed for normality. In the spatial interpolation, the kriging variance map was therefore automatically calculated on the logit-transformed scale. In order to present the prediction uncertainty, the kriging variance map needed to be back-transformed to the original data scale. In the former manuscript, a simple process using the inverse logit equation (Eq.14 in Hengl et al. 2004) was applied, and it ignored the best linear unbiased estimator principle and resulted in unreasonable kriging variance values.

In this revised manuscript, a transGaussian kriging algorithm adopted from Cressie (1993) was used to compute the kriging variance and the kriging standard deviation. The recalculated kriging variance map had no extremely high numbers this

time, and therefore the kriging standard deviation, shown in Figure 10 in this revised manuscript, was comparable to the order of magnitude of the predicted N₂O fluxes presented in Figure 9.

References

Hengl, T., Heuvelink, G.B.M., and Stein, A.: A generic framework for spatial prediction of soil variables based on regression-kriging, *Geoderma*, 120, 75-93, 2004.

Cressie, N.A.C.: *Statistics for Spatial Data*, Wiley, 1993.

Author's Changes to the Manuscript:

In Figure 10, the kriging variance map was replaced with the kriging standard deviation map. Please see P49 in the revised manuscript.

2) line 88: better write: "...of the interannual variability of N₂O emissions..."

Author's Response:

Corrected.

Author's Changes to the Manuscript:

The sentence in L87-89 was changed to "To obtain a more accurate evaluation of the interannual variability of N₂O emissions from tea-planted soils, a study on the spatial structure and distribution of N₂O emissions during a wet season (in contrast to the dry

season) is necessary.”. Please see the change in P5 L87-90 in the revised manuscript.

3) you wrote: line 291: "The kriging error maps were showed in Fig. 10, also indicating the CK method outperforming the other spatial interpolation methods."

To my opinion, this is not visible in Figure 10. Can you please explain which features in Figure 10 c+d show that CK outperforms the other methods?

Author's Response:

In the revised manuscript, the kriging variance map was changed to the kriging standard deviation map shown in Figure 10. For the four kriging interpolations of OK, RK, CK with SOCt as the covariable and CK with NH4Nt and NO3Nt as the covariables, the kriging standard deviations of CK and RK were obviously lower than that of OK, indicating that CK and RK outperformed the OK method. For the performance of CK and RK, it is hard to distinguish them by eye. However, shown in Table 4 regarding kriging cross validation, the CK method had lower root mean squared errors (RMSE) and higher correlation coefficient (r) values than the RK method, indicating a better performance.

Author's Changes to the Manuscript:

The sentence “The kriging error maps were showed in Fig. 10, also indicating the CK method outperforming the other spatial interpolation methods.” in P14 L288-289 was changed to “The kriging standard deviation maps were showed in Fig. 10, and clearly

indicated that the RK and CK methods with lower kriging standard deviations outperformed the OK method with higher kriging standard deviations.”. Please see P14 L288-290 in the revised manuscript.

4) The caption for Figure 10 can be shortened as it is the same as Figure 9, just reflecting the kriging error.

Author’s Response:

Corrected.

Author’s Changes to the Manuscript:

The new caption of Figure 10 was “Figure 10. Spatial distributions of kriging standard deviations of the predicted N₂O fluxes by (a) OK, (b) RK, (c) CK with SOCt as the covariable, and (d) CK with NH₄Nt and NO₃Nt as two covariables.”. Please see P39 L672-674 in the revised manuscript.

1 Wet-season spatial variability of N₂O emissions from a tea field in subtropical central China

2

3 Xiaoqing Fu, Xinliang Liu, Yong Li *, Jianlin Shen, Yi Wang, Ganghua Zou, Hang Li, Lifang

4 Song, Jinshui Wu

5

6 Changsha Research Station for Agricultural & Environmental Monitoring and

7 Key Laboratory of Agro-ecological Processes in Subtropical Regions,

8 Institute of Subtropical Agriculture, Chinese Academy of Sciences,

9 Hunan 410125, China

10 These two authors contributed equally to this work.

11 *Correspondence to: Professor Yong Li

12 Institute of Subtropical Agriculture,

13 Chinese Academy of Sciences, Hunan 410125, China

14 Tel: +86-731-8461-5291

15 Fax: +86-731-8461-2685

16 E-mail: yli@isa.ac.cn

17

18 **Abstract**

19 Tea fields emit large amounts of nitrous oxide (N₂O) to the atmosphere. Obtaining accurate
20 estimations of N₂O emissions from tea-planted soils is challenging due to strong spatial
21 variability. We examined the spatial variability of N₂O emissions from a red-soil tea field in
22 Hunan province, China, on 22 April 2012 (in a wet season) using 147 static mini chambers
23 approximately regular gridded in a 4.0 ha tea field. The N₂O fluxes for a 30-min snapshot
24 (10:00-10:30 am) ranged from -1.73 to 1,659.11 g N ha⁻¹ d⁻¹ and were positively skewed with
25 an average flux of 102.24 g N ha⁻¹ d⁻¹. The N₂O flux data were transformed to a normal
26 distribution by using a logit function. The geostatistical analyses of our data indicated that the
27 logit-transformed N₂O fluxes (FLUX30t) exhibited strong spatial autocorrelation, which was
28 characterized by an exponential semivariogram model with an effective range of 25.2 m. As
29 observed in the wet season, the logit-transformed soil ammonium-N (NH₄Nt), soil nitrate-N
30 (NO₃Nt), soil organic carbon (SOct), total soil nitrogen (TSNt) were all found to be
31 significantly correlated with FLUX30t ($r=0.57-0.71$, $p < 0.001$). Three spatial interpolation
32 methods (ordinary kriging, regression kriging and cokriging) were applied to estimate the
33 spatial distribution of N₂O emissions over the study area. Cokriging with NH₄Nt and NO₃Nt
34 as covariables ($r=0.74$ and RMSE=1.18) outperformed ordinary kriging ($r=0.18$ and
35 RMSE=1.74), regression kriging with the sample position as a predictor ($r=0.49$ and
36 RMSE=1.55) and cokriging with SOct as a covariable ($r=0.58$ and RMSE=1.44). The
37 predictions of the three kriging interpolation methods for the total N₂O emissions of 4.0 ha
38 tea field ranged from 148.2 to 208.1 g N d⁻¹, based on the 30 min snapshots obtained during

39 the wet season. Our findings suggested that to accurately estimate the total N₂O emissions
40 over a region, the environmental variables (e.g., soil properties) and the current land use
41 pattern (e.g., tea row transects in the present study) must be included in spatial interpolation.
42 Additionally, compared with other kriging approaches, the cokriging prediction approach
43 showed great advantages in being easily deployed, and more importantly providing accurate
44 regional estimation of N₂O emissions from tea-planted soils.

45

46 **Introduction**

47 According to the latest data, which show rapid increases in their atmospheric concentrations
48 (IPCC, 2013), nitrous oxide (N₂O), carbon dioxide (CO₂) and methane (CH₄) are three major
49 greenhouse gases in the atmosphere that significantly contribute to global warming. Among
50 these major greenhouse gases, N₂O has a very high radiative forcing per unit mass (265-fold
51 stronger than CO₂ on a 100 year horizon) and plays an important role in ozone depletion in
52 the stratosphere (Ravishankara et al., 2009). The primary sources of N₂O are from agriculture
53 development and the subsequent increased use of chemical N fertilizers (Ambus and
54 Christensen, 1994; Mosier et al., 1996, 1998; Yanai et al., 2003; Tokuda and Hayatsu, 2004;
55 Akiyama et al., 2006; Ravishankara et al., 2009). Agricultural soils produce 2.8 (1.7–4.8) Tg
56 of N₂O-N yr⁻¹ (IPCC, 2013). The N₂O is emitted from soils via the microbial processes of
57 nitrification under aerobic conditions and denitrification under anaerobic conditions
58 (Firestone and Davidson, 1989; Wrage et al., 2004). The magnitude of soil N₂O emissions is
59 highly variable and strongly influenced by changes in environmental conditions.

60 Among the different agricultural soils, tea-planted soils are important sources of N₂O that
61 are rapidly attracting attention due to recent large increases in the number of tea plantations
62 and large N fertilizer inputs (Akiyama et al., 2006; Lin and Han, 2009; Fu et al., 2010, 2012;
63 Hirono and Nonaka, 2012; Han et al., 2013; Li et al., 2013). In China, the total tea-planted
64 area was approximately 2.10 million ha (mostly distributed in Fujian, Anhui, Zhejiang and
65 Hunan) in 2013 (NBSC, 2014). Compared with other agricultural soils, tea-planted soils
66 provide optimal conditions (e.g., low soil pH, high temperature and ample moisture) for
67 microbes to emit significant amounts of N₂O (Hayatsu, 1993; Venterea and Rolston, 2000; Li
68 et al., 2013). However, because few measurements of N₂O emissions from tea-planted soils
69 have been reported in China (Fu et al., 2012; Li et al., 2013; Han et al., 2013), it is difficult to
70 conduct precise spatial and temporal evaluations of N₂O emissions from tea-planted soils. To
71 estimate the N₂O emissions from tea-planted soils accurately and to understand the roles that
72 tea plantations play in global warming, it is necessary to investigate the spatial and temporal
73 patterns and related mechanisms of N₂O emissions from tea fields. This information will lead
74 to the development of effective land management options for mitigating N₂O emissions from
75 a significant source, tea plantation.

76 The N₂O fluxes have large spatial variability in agricultural soils (Konda et al., 2008,
77 2010; Meda et al., 2012; Li et al., 2013). Many previous studies in tea fields have found
78 pronounced seasonal fluctuations in N₂O fluxes, with higher N₂O emissions during the wet
79 season than during the dry season (Fu et al., 2012; Han et al., 2013). The seasonal and spatial
80 variability of N₂O emissions significantly contributes to the uncertainty when estimating the

81 contributions of subtropical tea-planted ecosystems to N₂O flux. Moreover, most of our
82 knowledge regarding seasonal changes and the spatial variability of N₂O fluxes is based on a
83 small number of measurements taken from tea-planted soils. [Li et al. \(2013\)](#) investigated the
84 spatial structure of N₂O fluxes for tea-planted soils during the dry season in October 2010
85 and found that the spatial distribution of the N₂O fluxes was primarily associated with field
86 elevation ($r=-0.42$, $p<0.001$). The other soil properties (e.g., soil organic carbon, soil water
87 and soil mineral nitrogen) were not significantly related to N₂O flux. To obtain a more
88 accurate evaluation of the interannual variability of N₂O emissions from tea-planted soils, a
89 study on the spatial structure and distribution of N₂O emissions during a wet season (in
90 contrast to the dry season) is necessary.~~To obtain a more accurate evaluation of annual N₂O~~
91 ~~emissions from tea-planted soils, a study on the spatial structure and distribution of N₂O~~
92 ~~emissions during a wet season (in contrast to the dry season) is necessary.~~

93 To understand the structure of the spatially distributed data and to predict the N₂O fluxes
94 at the unsampled locations, geostatistical analyses can be useful ([Goovaerts, 1997](#); [Webster](#)
95 [and Oliver, 2001](#)). Geostatistics provide statistical tools for describing the quantitative spatial
96 variability of field observations for the accurate mapping and planning of rational sampling
97 schemes that efficiently utilize the available labor ([Webster, 1985](#)). Several geostatistical
98 methods are used to examine the spatial variability of N₂O fluxes, including simple kriging
99 (SK), ordinary kriging (OK), regression kriging (RK) and cokriging (CK). The most
100 commonly used method is OK ([Clemens et al., 1999](#); [Röver et al., 1999](#); [Mathieu et al., 2006](#);
101 [Konda et al., 2008, 2010](#)), which uses the derived theoretical semivariogram models to

102 interpolate the spatial distribution of N₂O fluxes. However, research has demonstrated that
103 RK and CK approaches, which use related auxiliary variables, improve the prediction
104 accuracy (Goovaerts, 1997; Webster and Oliver, 2001; Hengl et al., 2004). The RK method
105 combines multiple regressions, including linear regressions, generalized linear models,
106 generalized added models and regression tree models, with the auxiliary variables used for
107 kriging (Odeh et al., 1994). In the RK method, linear regressions are commonly used. The
108 CK approach uses correlations that may exist between the predicted variables and other more
109 easily measured variables. These variables can be measured at the same points as the
110 predicted variable, at other points, or at both. Compared with the RK approach, the CK
111 approach is commonly applied when the measurement of a covariable is less expensive than
112 the cost of a predicted variable (Stein et al., 1988; Odeh et al., 1995). In addition to the
113 feature correlation as a criterion for selecting covariables, the CK approach also requires that
114 both of the predicted variable and covariables have similar spatial structures (Odeh et al.,
115 1994). In this study, we used three interpolation methods (OK, RK and CK) to estimate the
116 spatial distribution of N₂O fluxes in a tea field.

117 In contrast with the dry season, the spatial variability of the N₂O emissions was
118 investigated during the wet season in April 2012 from the same tea-planted catchment that
119 was studied by Li et al. (2013). The catchment consisted of a completely independent
120 hydrological system. Thus, the spatial distribution of the N₂O emissions within the catchment
121 was expected to have intrinsic characteristics. The objectives of this study were to (i) evaluate
122 the spatial variability of N₂O emissions from soils planted with tea in subtropical central

123 China during the wet season, (ii) determine the key environmental factors controlling N₂O
124 emissions, and (iii) assess the prediction efficiency of three kriging interpolation methods.
125

126 **2. Materials and Methods**

127 *2.1 Site description*

128 The field experiment was conducted in a small catchment (4.0 ha) in Jinjing, Changsha, in
129 Hunan province, China (28°32'50"N and 113°19'58" E and elevation 90 to 111 m) (Fig. 1).
130 The region has a subtropical monsoon climate with a mean annual air temperature of 17.5°C
131 and a mean annual precipitation of 1400 mm (average from 1979 to 2012). The site had four
132 distinct seasons: spring (February to April), summer (May to July), autumn (August to
133 November), and winter (December to January). On average, 70% of the annual precipitation
134 occurred in April, May and June. The daily air temperature and precipitation for 2012 were
135 recorded by an automatic weather station (Intelimet A, IMET-ADV2, Dynamax, USA)
136 located next to the studied catchment (Fig. 2). The soil of the catchment was a Haplic Alisol
137 (FAO/UNESCO soil taxonomy) that was derived from a granitic parental material. Tea
138 (*Camellia sinensis L., cv. Baihaozao*) was contour-planted 10 years ago using an inter-row
139 spacing of 0.5 m in the catchment.

140

141 <Insert Fig. 1 & Fig. 2 near here>

142

143 *2.2 Sampling positions*

144 In the 4.0 ha tea-planted catchment, 1964 evenly-distributed points with plane coordinates
145 and elevation values and 456 centerlines of tea tree row were recorded by locally calibrated
146 differential Geographic Positioning System (DGPS) receiver (Sanding Southern Survey Co.,
147 China), and then were used to develop the local DEM and land use data (at a spatial
148 resolution of 0.1 m, respectively, as shown in [Fig. 1c and d](#)). The land use data showed the
149 four positions where the chambers were placed, including the inter-row, fertilization point,
150 under tea tree and in tea tree row, as described in [Li. et al. \(2013\)](#). The spatial positions of the
151 gas sampling points in a 15 m × 15 m regular grid over the catchment were originally
152 determined using a DGPS receiver on 20 April 2012. Some of the chamber positions were
153 slightly adjusted (because of a lack of space in the tea tree rows or to avoid roads and
154 trenches). Thus, the chambers were placed in one of four locations mentioned above ([Fig. 1d](#)).
155 Overall, 147 sampling points were determined, and the Euclidean distances between each
156 point and its nearest neighbors ranged from 14.6 m to 16.7 m. The x-y coordinates, the gas
157 sampling position information (the inter-row, fertilization point, under tea tree and in tea tree
158 row along tea row transects), and the elevations at the sampling points were recorded.

159

160 *2.3 Gas and soil properties measurements*

161 Gas and soil samples were collected at each grid point on 22 April 2012 using a closed mini
162 chamber technique. A mini chamber set was composed of PVC and had two parts (base and
163 chamber). The base was 0.15 m in diameter and 0.05 m high. The chamber was 0.15 m in
164 diameter and 0.15 m high, and was equipped with rubber septa on the top for gas sampling. In

165 the field operation, the base was gently inserted vertically into the soil on 20 April 2012, and
166 the chamber was clipped on the base with the sponge seals in between to stop gas leaking
167 before gas sampling on 22 April 2012. Therefore, the effective static chambers volume was
168 equal to the chamber volume of 0.002651 m³. Gas samples were collected from the
169 headspace between 10:00 and 10:30 am. For simultaneous sampling, 25 skilled gas sampling
170 persons helped to accomplish the field sampling. Each person only took care of one column
171 containing 4 to 8 sampling positions (see [Fig. 1](#)), and started sampling at the same time of 10
172 am. At each point, three gas sample replicates were collected from the headspace into
173 pre-evacuated 12 mL vials (Exetainers, Labco, UK) at 0 and 30 min after the chamber body
174 was clipped. After collecting the gas samples, the air temperature in each chamber was
175 measured for subsequent correction of the flux calculation, and then three replicate soil cores,
176 0.05 m in diameter and 0.20 m in depth, were collected from the soils inside the mini
177 chambers. Soil samples were put straight into clean zip-lock bags for avoiding soil moisture
178 loss, and quickly transported back to the laboratory in thermal insulation boxes and stored in
179 a refrigeration room at 4 °C for preventing any microbial activity (such as mineralization,
180 nitrification and denitrification). The N₂O concentrations of the gas samples were analyzed
181 using a gas chromatograph (Agilent 7890A, Agilent, USA) that was fit with a ⁶³Ni-electron
182 capture detector and an automatic sample injector system. The N₂O fluxes (FLUX30, g N ha⁻¹
183 d⁻¹) were calculated as described by Li et al. (2013). The soil physical/chemical properties
184 determined by using fresh soil, e.g., the soil ammonium content (NH₄N), soil nitrate content
185 (NO₃N), soil dissolved organic carbon content (DOC), soil volumetric water content (SWC),

186 and soil bulk density (BD), were measured within three days after sampling, while those
187 using air-dried soil, e.g., total soil nitrogen content (TSN), soil organic carbon content (SOC)
188 and soil clay/silt/sand content (CLAY, SILT and SAND), were determined within two weeks
189 after the field work.

190

191 *2.4 Data analyses*

192 The descriptive statistical and geostatistical analyses were performed using R ([R](#)
193 [Development Core Team, 2014](#)) with the *gstat* package ([DGUU, 2010](#)).

194 Descriptive statistical analyses were used to determine the mean, median, minimum and
195 maximum values, SD, coefficient of variation (CV), and skewness of the original and
196 logit-transformed data. These analyses were based on the four chamber placement positions.
197 Because the FLUX30, NH₄N, NO₃N, SOC, TSN and SWC data were highly skewed, these
198 values were transformed by using a logit function ([Hengl et al., 2004](#)). The transformed
199 variables were named FLUX30t, NH₄Nt, NO₃Nt, SOct, TSNt and SWCt. Using a Pearson's
200 correlation, the relationships between FLUX30t, NH₄Nt, NO₃Nt, SOct, TSNt, SWCt, DOC,
201 BD, SAND, SILT, and CLAY were tested. The significance of the differences in the FLUX30t
202 and environmental factors (NH₄Nt, NO₃Nt, SOct, TSNt and DOC) between any two of the
203 different chamber positions along the entire tea-tree row transect were evaluated using the
204 Tukey's Honest Significant Difference method.

205 In the geostatistical analyses, an experimental semivariogram of FLUX30t was
206 calculated, and the theoretical semivariogram models were fit. The ratio of the partial sill to

207 the total sill was used as an index of spatial dependence. [Armstrong \(1998\)](#) stated that a
208 variable with a higher ratio of partial sill to sill and a longer semivariogram range were more
209 structured. The spatial distribution of FLUX30t across the catchment was predicted using
210 three kriging interpolation methods (OK, RK and CK). These data were transformed back to
211 the original scale of FLUX30 for mapping. The Leave-One-Out cross-validation method was
212 used to evaluate the accuracy of interpolating FLUX30t using the three different kriging
213 methods.

214

215 **3. Results**

216 *3.1 Exploratory data analyses*

217 In the 4.0 ha tea-planted catchment, the N₂O fluxes during the 30-min one-time
218 measurements performed on 22 April 2012 ranged from -1.73 to 1,659.11 g N ha⁻¹ d⁻¹, with a
219 median value of 27.56 g N ha⁻¹ d⁻¹ and a CV of 234.7 % ([Table 1](#)). The N₂O flux data were
220 positively skewed ([Table 1 and Fig. 3a](#)), and their logit-transformations were approximately
221 normally distributed ([Table 1 and Fig. 3b](#)). From [Table 3](#), the logit-transformed N₂O fluxes
222 (FLUX30t) were the highest in the fertilization points, and the differences in the FLUX30t
223 values among the chamber placement positions were statistically significant ($p < 0.001$).

224

225 *<Insert Table 1 & Fig. 3 near here>*

226

227 The ELEVATION, BD, DOC, SWC, SAND, SILT, and CLAY were approximately
228 normally distributed, with skewness values of less than 1 (Table 1). Additionally, DOC
229 displayed a moderate CV of 34.6 %, and the other variables had lower CVs (4.1–23.8 %). The
230 NH₄N, NO₃N, SOC and TSN were positively skewed, and the logit-transformations (NH₄Nt,
231 NO₃Nt, SOct and TSnt) had approximately normal distributions (Table1). The NH₄N and
232 NO₃N had very high CVs (190.8 % and 141.6 %, respectively), and the SOC and TSN had
233 moderate CVs (50.1 % and 38.3 %, respectively).
234 The NH₄Nt, NO₃Nt, SOct, TSnt and SWC were significantly correlated with the N₂O fluxes
235 (Fig. 5), and the NH₄Nt, NO₃Nt and TSnt had strong positive relationships with N₂O ($r =$
236 0.71, 0.70 and 0.57, respectively, $p < 0.001$). The N₂O emissions and some soil properties
237 (NH₄N, NO₃N, SOC, TSN and SWC) in the fertilization points were significantly different
238 ($p < 0.001$) from the other three chamber placement positions (Fig. 6). These variables were
239 used as auxiliary covariables for the CK approach.

240

241 <Insert Fig. 4 & Fig. 5 near here>

242

243 3.2 Spatial variability of N₂O emissions and related environmental factors

244 Because most of the soil properties were significantly correlated with the chamber placement
245 positions, two types of semivariogram models were calculated for the N₂O and soil
246 parameters (correlated with N₂O fluxes) in the wet season (Table 2). The FLUX30t exhibited
247 strong spatial autocorrelation and was characterized by an exponential semivariogram model,

248 a theoretical distance parameter of 8.40 m (equivalent to an effective range of 25.2 m) and a
249 zero nugget. The NH₄Nt, SWCt, SAND and SILT showed almost no spatial dependency,
250 while NO₃Nt and TSNt demonstrated weak spatial dependency with a range parameter of
251 91.9 and 58.0 m, respectively (equivalent to an effective range of 163.7 and 102.6 m,
252 respectively). The SOCt exhibited a moderate spatial dependency within 93.0 m. By
253 detrending the influence of the chamber placement position, large changes in the
254 semivariogram models occurred regarding the above variables. Although the semivariograms
255 of the regression residuals of FLUX30t, NH₄Nt, NO₃Nt and SOCt were best-fit with the
256 same semivariogram model (exponential) with a similar range of 17.4 m (equivalent to an
257 effective range of 52.1 m), the spatial dependencies of those variables were different (Table
258 2). Of the soil properties, only SOCt had a similar spatial structure to FLUX30t when the
259 influence of the chamber placement position was detrended (Table 2). Based on these
260 correlation analyses and spatial variability analyses, the covariables for the CK method were
261 determined.

262

263 *<Insert Table 2 near here>*

264

265 3.3 Spatial interpolation of N₂O emissions by three methods

266 Three spatial interpolation methods were used in this study to predict the spatial distribution
267 of N₂O emissions from tea soils in the catchment. In the first method, the derived theoretical
268 semivariogram model for FLUX30t that is presented in Table 2 was used for the OK

269 prediction. In the second method, RK was used and the chamber placement position was
270 identified as the auxiliary regression predictor. Thus, the semivariogram of the regression
271 residuals of FLUX30t were calculated and best-fit with the theoretical semivariogram model
272 shown in Fig. 6. In the third method, CK involved two groups of covariables. As described
273 previously, because SOct (detrending the influence of chamber placement position) showed a
274 similar spatial structure to FLUX30t (detrending the influence of chamber placing position), a
275 CK process was performed using SOct as the covariable. Firstly, the direct and
276 cross-semivariograms of FLUX30t and SOct (detrending the influence of the chamber
277 placement position) were calculated and best-fit with a linear model for co-regionalization
278 (LMC). Next, the fitted LMC was used to predict the spatial surface of N₂O emissions.
279 Because NH₄Nt and NO₃Nt were significantly correlated with FLUX30t (Fig. 5), a second
280 CK with NH₄Nt and NO₃Nt as the covariables was processed, similarly to that of the CK
281 with SOct. However, these covariables had different spatial structures (Table 2). As reflected
282 by the lower root mean squared error (RMSE) and higher *r* values (Table 4), the CK method
283 performed better than the other spatial interpolation methods. Furthermore, the CK with
284 NH₄Nt and NO₃Nt as two covariables outperformed the CK with SOct as the covariable.

285

286 *<Insert Figs.6-9 near here>*

287

288 As shown in Fig. 9, the surface map for the spatial distribution of N₂O emissions
289 interpolated by OK was rougher than the maps obtained from the other interpolation

290 approaches. The kriging standard deviation maps were showed in Fig. 10, and clearly
291 indicated that the RK and CK methods with lower kriging standard deviations outperformed
292 the OK method with higher kriging standard deviations.~~The kriging error maps were showed~~
293 ~~in Fig. 10, also indicating the CK method outperforming the other spatial interpolation~~
294 ~~methods.~~ –The four kriging interpolations of OK, RK, CK with SOCt as the covariable and
295 CK with NH4Nt and NO3Nt as the covariables were able to predict that the total amount of
296 N₂O emissions in the tea fields during the wet season were 208.1 g N d⁻¹, 148.2 g N d⁻¹, 149.7
297 g N d⁻¹ and 150.5 g N d⁻¹, respectively. From the performance evaluations of the four spatial
298 interpolations, the total N₂O emissions from the tea field on 22 April 2012 during the wet
299 season were approximately 150 g N d⁻¹.

300

301 <Insert Fig. 10 near here>

302

303 Discussion

304 4.1 Seasonal differences of N₂O fluxes in the red soil planted with tea

305 The N₂O emissions from soils have obvious seasonal fluctuations, with emissions that are
306 significantly higher during the wet season than during the dry season (Konda et al., 2010). To
307 understand the seasonal changes in the spatial structures of N₂O fluxes, we compared the
308 N₂O emissions between the wet (this study) and dry (Li et al., 2013) seasons. In general, the
309 mean, SD and coefficient of variation (102.24, 239.96 g N ha⁻¹ d⁻¹ and 234.7 %, respectively)
310 of the N₂O fluxes in the wet season were all higher than those (2.88, 8.94 g N ha⁻¹ d⁻¹ and
311 152.0 %, respectively) during the dry season (Table 3). Furthermore, in contrast with the dry

312 season, the N₂O fluxes during the wet season were significantly different among the four
313 chamber placement positions, with the highest fluxes occurring at the fertilization points and
314 the inter-row positions (Table 3). During the wet season, the high N₂O fluxes at the
315 fertilization points and the inter-row positions resulted from the high soil moisture, due to
316 more rainfall, and from the fertilization that occurred on 19 February 2012 (Fig. 2). The soil
317 N and the soil organic C availability are directly increased by the application of chemical and
318 organic N fertilizers. The additional in the available C and N supplied by fertilization resulted
319 in increased soil microbial activity, which stimulated the nitrification and denitrification
320 processes that contribute to soil N₂O emissions (Davidson et al., 1993; Kiese et al., 2003;
321 Werner et al., 2007).

322

323 *<Insert Table 3 near here>*

324

325 4.2 Spatial structure of N₂O emissions from red soils planted with tea

326 Soil type, topography and land management (fertilization, tillage and irrigation) are the
327 primary factors that affect the spatial structures of N₂O emissions (Folorunso and Rolston,
328 1984; Clemens et al., 1990; Velthof et al., 1996; Konda et al., 2008). During the wet season,
329 the N₂O fluxes showed a strong spatial dependence (with a range of approximately 25.3 m)
330 that was similar to the dry season range of approximately 28.0 m in the tea-planted fields (Li
331 et al., 2013). These results indicated that the spatial dependence of N₂O fluxes at the current
332 spatial sampling scale was comparable between seasons. Our findings for a fertilized tea field

333 were similar to those of [Konda et al. \(2010\)](#) for a tropical forest. However, these results
334 contrasted those of many previous investigations for agricultural fields, including winter
335 wheat ([Ball et al., 1997](#); [Clemens et al., 1999](#); [Röver et al., 1999](#); [Mathieu et al., 2006](#)),
336 summer maize ([Clements et al., 1999](#)), onion ([Yanai et al., 2003](#)), and grassland ([Ambus and](#)
337 [Christensen, 1994](#); [Velthof et al., 1996](#); [van den Pol-van Dasselaar et al., 1998](#); [Turner et al.,](#)
338 [2008](#)) fields, in which the N₂O flux presented no, weak or moderate spatial dependence. This
339 discrepancy primarily occurred because of the unique geographical characterization and land
340 management of the tea plantation. Compared with other agricultural fields in flat areas, tea
341 fields are always distributed in hills or mountains. Therefore, the contributions of the
342 topography to the spatial dependence of the N₂O flux were strong ([Li et al., 2013](#)).
343 Additionally, tea is a perennial plant. Thus, apart from fertilization and weeding, the soil
344 disturbance in tea fields is always very low.

345 During the dry season, the topography (elevation) had a significant effect on the spatial
346 pattern of N₂O fluxes in the tea-planted fields ([Li et al., 2013](#)). Similar spatial patterns of N₂O
347 fluxes with topography were also observed in forest soils ([Van Kessel et al., 1993](#); [Konda et](#)
348 [al., 2010](#)). Theoretically, the SWC varies with the topography and affects the spatial pattern
349 of N₂O fluxes by controlling the conditions for soil nitrification and denitrification ([Firestone](#)
350 [and Davidson, 1989](#); [Wrage et al., 2004](#)). Although the SWC had no relationships with N₂O
351 and elevation during the dry season ([Li et al., 2013](#)), a correlation existed in the present study
352 ([Fig. 5](#)). The microstructures of the tea tree-row transect and the land management practices
353 of tea production were the primary influences on the spatial pattern of soil water in the

354 tea-planted fields (Li et al., 2013). During the wet season, fertilization contributed to the
355 spatial pattern of N₂O fluxes in the tea-planted fields, with the highest averaged fluxes at the
356 fertilization sites (198.81 g N ha⁻¹ d⁻¹) (Table 3). Fertilization resulted in similar spatial
357 patterns of N₂O fluxes in other agricultural soils (Ball et al., 1997; Clements et al., 1999;
358 Röver et al., 1999; Mathieu et al., 2006; Yanai et al., 2003).

359 In view of the analysis of the primary factors that affected the spatial pattern of N₂O
360 fluxes, we detrended the influences of the environmental factors when the N₂O flux
361 semivariograms were calculated to more deeply explore the spatial structures of the N₂O
362 emissions in the tea-planted fields. For example, during the dry and wet seasons, the spatial
363 influences of elevation (Li et al., 2013) and chamber placement position, respectively, were
364 detrended when computing the N₂O flux semivariograms. Because the relationship between
365 chamber placement position and N₂O flux was more relevant than the relationship between
366 elevation and N₂O flux, the effect of detrending the influence of chamber placement position
367 during the wet season was more obvious than that of detrending the influence of elevation
368 during the dry season (Li et al., 2013). This effect was also reflected in the evaluation of the
369 performance of the RK method for the wet and dry seasons (Table 4).

370

371 *4.3 Spatial interpolations of N₂O emissions by three methods*

372 The three interpolation methods (OK, RK and CK) were used to predict the spatial
373 distributions of N₂O emissions from the red soils planted with tea during dry (Li et al., 2013)
374 and wet seasons (this study). However, these three methods resulted in significantly different

375 performances between the dry and wet seasons (Table 4). We conducted comparative
376 analyses for the performance of the three interpolation methods using two aspects: different
377 seasons and different methods. Firstly, the OK method performed better when predicting the
378 spatial distribution of N₂O fluxes for the dry season relative to the wet season. Because the
379 OK method directly used the fitted theoretical semivariogram model of the target variable to
380 predict the spatial distribution, its performance reflected the predictive ability of the original
381 data (Goovaerts, 1997). During the wet season, more factors (e.g., NH₄N, NO₃N, SOC, TSN
382 and SWC) influenced the spatial distributions of the N₂O fluxes than the dry season (Table 2
383 and Fig. 5). The values of the original data were concealed. Thus, other sophisticated kriging
384 methods, such as RK and CK, which reconcile the relationships between N₂O fluxes and
385 environmental factors, could be useful. The RK method performed better when elevation was
386 used as an auxiliary regression predictor during the dry season than when the chamber
387 placement position was used during the wet season (Table 4). This finding primarily occurred
388 because the chamber placement position was a categorical variable with a lower regression
389 fitting ability than elevation, which was a continuous variable (Goovaerts, 1997). The
390 performances of the CK with two groups of covariables during the wet season were better
391 than those of the CK with three groups of covariables during the dry season (Table 4).
392 Particularly, the CK with strongly correlated covariables of NO₃N and NH₄N ($r = 0.70-0.71$
393 and $p < 0.001$) (Fig. 5) performed the best ($r = 0.74$ and $RMSE = 1.04$) (Table 4).

394 Secondly, by comparing the performances of the three interpolation methods, the RK and
395 CK methods, which are more sophisticated kriging technologies, performed better than the

396 OK method for the dry and wet seasons. Similar results were obtained by previous
397 researchers (Stein et al., 1988; Odeh et al., 1995; Goovaerts, 1997; Hengl et al., 2004). When
398 comparing the performances of RK and CK, no differences were observed for the dry season.
399 However, during the wet season, the CK significantly outperformed the RK (Table 4). Overall,
400 few attempts have been made to provide a good method for selecting interpolation methods
401 between RK and CK (Kontters et al., 1995; Odeh et al. 1995). Li et al. (2013) suggested that
402 RK was a good choice because of the performance of the two interpolation methods and the
403 difficulties encountered when applying CK. However, in this study, the CK method was
404 better than the RK method because of its high predictive performance (Table 4), its readily
405 available required covariables (e.g., NH₄N, NO₃N and SOC) at co-locations, and because
406 expensive surface data were not needed (e.g., DEM and land use data, which are required by
407 RK) (Goovaerts, 1997; Webster and Oliver, 2001). Our conclusions were similar to those of
408 many previous studies that found that CK was the most versatile and rigorous statistical
409 technique for estimating spatial points (Stein et al., 1988; Odeh et al., 1995; Webster and
410 Oliver, 2001). For the application of CK, the covariables must show a correlation with the
411 target variable and present a similar spatial structure as the target variable (Odeh et al., 1995;
412 Goovaerts, 1997; Webster and Oliver, 2001). Therefore, we further compared the effects of
413 the two groups of covariables for CK in this study. We found that CK method with NH₄Nt
414 and NO₃Nt (showed significant correlations with FLUX30t) as covariables outperformed the
415 CK method with SOCt (presented a similar spatial structure to FLUX30t) as a covariable,
416 indicating that the feature correlation was more important than the similarity of the spatial

417 structure when selecting CK covariables. This finding can be regarded as a prerequisite for
418 selecting covariables for CK application.

419

420 *<Insert Table 4 near here>*

421

422 The three spatial interpolation methods predicted similar total N₂O emissions from the
423 tea-planted red soils in the 4.0 ha catchment on 30 October 2010 (in the dry season) and on
424 22 April 2012 (in the wet season), ranging from 21.2 to 22.1 g N d⁻¹ and from 148.2 to 208.1
425 g N d⁻¹ (Table 4), respectively. The predicted errors during the wet season were higher than
426 those of the dry season (Table 4). This result mainly occurred because fertilization was a
427 major factor that affected the N₂O emissions from the tea fields during the wet season.
428 Following fertilization, the horizontal and vertical movement of NH₄N and NO₃N in the
429 topsoil of the tea fields potentially produced the strong spatial heterogeneity of N₂O
430 emissions. In addition, it is possible that the variations in the availability of oxygen in the
431 soils was regulated by soil moisture, which determined the spatio-temporal heterogeneity of
432 N₂O emissions by inducing different degrees of soil nitrification and denitrification
433 (Davidson et al., 2000; Konda et al., 2010). Thus, spatial interpolation methods must be
434 chosen carefully to accurately estimate the spatial distribution of N₂O emissions when the
435 emissions are high and have strong spatial variability in the fields.

436

437 **5 Conclusions**

438 During the wet season of 2012, a 30-min one-time measurement of N₂O emissions from a 4.0
439 ha red-soil tea field in the subtropical region of central China were determined at 147 points.
440 The N₂O fluxes significantly varied with space. In addition, the N₂O fluxes were significantly
441 correlated with the NH₄N, NO₃N, SOC and TSN contents ($r > 0.27$ and $p < 0.001$). The
442 logit-transformed N₂O fluxes demonstrated a strong spatial dependency and were
443 characterized by an exponential semivariogram model with an effective range of 25.2 m.
444 Three spatial interpolation methods (OK, RK and CK) were used to predict the spatial
445 distribution of N₂O emissions. The RK and CK methods were relatively accurate for
446 predicting results. Although the N₂O emissions were much higher during the wet season than
447 in the dry season, the N₂O emissions exhibited similar spatial structure during both seasons.
448 Such a phenomenon was mainly attributed to the low soil disturbance (e.g., only fertilizing
449 in a very small proportion of area and weeding) in the tea field.

450 To effectively mitigate high N₂O emissions from the tea field soils, the biological and
451 chemical mechanisms of N₂O emissions must be deeply explored. In addition, the responsive
452 land management practices, such as biochar application, deep fertilization (under 20 cm), the
453 use of controlled-release fertilizers and ecological engineering, must be recommended and
454 deployed, especially during the wet season.

455

456 **Acknowledgements**

457 The National Basic Research Program of China (2012CB417105) and the National Natural
458 Science Foundation of China (41171200) financially supported this research.

459 **References**

- 460 Akiyama, H., Yan, X. Y., and Yagi, K.: Estimations of emission factors for fertilizer-induced
461 direct N₂O emissions from agricultural soils in Japan: Summary of available data, *Soil Sci.*
462 *Plant Nutr.*, 52, 774-787, 2006.
- 463 Ambus, P. and Christensen, S.: Measurement of N₂O emission from a fertilized grassland: an
464 analysis of spatial variability, *J. Geophys. Res.*, 99, 16557-16567, 1994.
- 465 Armstrong, M.: *Basic linear Geostatistics*, Springer Verlag, Berlin, 153 pp., 1998.
- 466 Ball, B. C., Horgan, G. W., Clayton, H., and Parker, J. P.: Spatial variability of nitrous oxide
467 fluxes and controlling soil and topographic properties, *J. Environ. Qual.*, 26, 1399-1409,
468 1997.
- 469 Clemens, J. Schillinger, M. P., Goldbach, H., and Huwe, B.: Spatial variability of N₂O
470 emissions and soil parameters of an arable silt loam - a field study, *Bio. Fert. Soils*, 28,
471 403-406, 1999.
- 472 Davidson, E. A., Matson, P. A., Vitousek, P. M., Riley, R., Dunkin, K., García-Méndez, G.,
473 and Maass, J. M.: Processes regulating soil emissions of NO and N₂O in a seasonally dry
474 tropical forest, *Ecology*, 74, 130-139, 1993.
- 475 Davidson, E. A., Keller, M., Erickson, H. E., Verchot, L. V., and Veldkamp, E.: Testing a
476 conceptual model of soil emissions of nitrous and nitric oxides, *Bioscience*, 50, 667-680,
477 2000.
- 478 DGUU (Department of Geography, Utrecht University): Introduction for Gstat, available at:
479 <http://www.gstat.org/index.html> (last access: 15 December 2010), 2010.

480 Firestone, M., and Davidson, E.: Microbial basis of NO and N₂O production and
481 consumption, in: Exchange of Trace Gases Between Ecosystems and the Atmosphere,
482 edited by: Andreae, M.O. and Schimel, D.S., John Wiley, Chichester, 7-21, 1989.

483 Folorunso, O. A., and Rolston, D. E.: Spatial variability of field measured denitrification gas
484 fluxes, *Soil Sci. Soc. Am. J.*, 48, 1214-1219, 1984.

485 Fu, X., Li, Y., Xiao, R., Tong, C., and Wu, J.: N₂O emissions from a tea field in subtropical
486 China. In: Proceedings of the 19th World Congress of Soil Science, Soil Solutions for a
487 Changing World, 1–6 August 2010, Brisbane (published on CDROM), 161-163, 2010.

488 Fu, X., Li, Y., Su, W., Shen, J., Xiao, R., Tong, C., and Wu, J.: Annual dynamics of N₂O
489 emissions from a tea field in southern subtropical China, *Plant Soil Environ.*, 58,
490 373-378, 2012.

491 Goovaerts, P.: *Geostatistics for Natural Resources Evaluation*, Oxford University Press, New
492 York, 483 pp., 1997.

493 Gorres, J. H., Dichiario, M. J., and Lyons, J. A.: Spatial and temporal patterns of soil
494 biological activity in a forest and an old field, *Soil Biol. Biochem.*, 30, 219-230, 1998.

495 Han, W. Y., Xu, J. M., Wei, K., Shi, W. Z., and Ma, L. F.: Estimation of N₂O emission from
496 tea garden soils, their adjacent vegetable garden and forest soils in eastern China, *Environ.*
497 *Earth Sci.*, 70, 2495-2500, 2013.

498 Hayatsu, M.: The lowest limit of pH for nitrification in tea soil and isolation of an acidophilic
499 ammonia oxidizing bacterium, *Soil. Sci. Plant Nutr.*, 39, 219-226, 1993.

500 Hengl, T., Heuvelink, G. B. M., and Stein, A.: A generic framework for spatial prediction of
501 soil variables based on regression-kriging, *Geoderma*, 120, 75-93, 2004.

502 Hirono, Y., and Nonaka, K.: Nitrous oxide emissions from green tea fields in Japan:
503 contribution of emissions from soil between rows and soil under the canopy of tea plants,
504 *Soil. Sci. Plant Nutr.*, 58, 384-392, 2012.

505 IPCC: Climate change 2013: the physical science basis. Contribution of working group I, in:
506 Fourth assessment report of the intergovernmental panel on climate change, edited by:
507 Solomon S., Qin D., Manning, M., Chen Z., Marquis, M., Averyt, K.B., Tignor, M.,
508 Miller, H.L., Cambridge University Press, Cambridge, 996 pp., 2013.

509 ISM (Institute for Statistics and Mathematics): The R Project for Statistical Computing,
510 available at: <http://www.r-project.org/> (last access: 15 December 2010), 2010.

511 Kiese, R., Hewett, B., Graham, A., and Butterbach-Bahl, K.: Seasonal variability of N₂O
512 emissions and CH₄ uptake by tropical rainforest soils of Queensland, Australia. *Global*
513 *Biogeochem. Cy.*, 17, 1043, doi:10. 1029/2002GB002014, 2003.

514 Konda, R., Ohta, S., Ishizuka, S., Arai, S., Ansori, S., Tanaka, N., and Hardjono, A.: Spatial
515 structures of N₂O, CO₂, and CH₄ fluxes from *Acacia mangium* plantation soils during a
516 relatively dry season in Indonesia, *Soil Biol. Biochem.*, 40, 3021-3030, 2008.

517 Konda, R., Ohta, S., Ishizuka, S., Heriyanto, J., and Wicaksono, A.: Seasonal changes in the
518 spatial structures of N₂O, CO₂ and CH₄ fluxes from *Acacia mangium* plantation soils in
519 Indonesia, *Soil Biol. Biochem.*, 42, 1512-1522, 2010.

520 Li, Y., Fu, X., Liu, X., Shen, J., Luo, Q., Xiao, R., Li, Y., Tong, C., and Wu, J.: Spatial
521 variability and distribution of N₂O emissions from a tea field during the dry season in
522 subtropical central China, *Geoderma*, 193, 1-12, 2013.

523 Lin, Y., and Han, W.: N₂O emissions from different soils, *Chinese Journal of Tea Science*, 29,
524 456-464, 2009.

525 Mathieu, O., Lévêque, J., Hénault, C., Milloux, M. J., Bizouard, F., and Andreux, F.:
526 Emissions and spatial variability of N₂O, N₂ and nitrous oxide mole fraction at the field
527 scale, revealed with ¹⁵N isotopic techniques, *Soil Biol. Biochem.*, 38, 941-951, 2006.

528 Meda, B., Flechard, C. R., Germain, K., Robin, P., Walter, C., and Hassouna, M.:
529 Greenhouse gas emissions from the grassy outdoor run of organic broilers,
530 *Biogeosciences*, 9, 1493-1508, doi:10.5194/bg-9-1493-2012, 2012.

531 Mosier, A. R., Duxbury, J. M., Freney, J. R., Heinemeyer, O., and Minami, K.: Nitrous oxide
532 emissions from agricultural fields: assessment, measurement and mitigation. *Plant Soil*,
533 181, 95-181, 1996.

534 Mosier, A. R., Kroeze, C., Nevison, C., Oenema, O., Seitzinger, S., and van Cleemput, O.:
535 Closing the global N₂O budget: nitrous oxide emissions through the agricultural nitrogen
536 cycle, *Nutr. Cycl. Agroecosys.*, 52, 225-248, 1998.

537 NBSC (a): China Statistical Yearbook, annual publication, National Bureau of Statistics of
538 China, Beijing, 2014.

539 Odeh, I. O. A., McBratney, A. B., and Chittleborough, D. J.: Spatial prediction of soil
540 properties from landform attributes derived from a digital elevation model, *Geoderma*, 63,
541 197-214, 1994.

542 Odeh, I. O. A., McBratney, A. B., and Chittleborough, D. J.: Further results on prediction of
543 soil properties from terrain attributes: heterotopic cokriging and regression kriging,
544 *Geoderma*, 67, 215-226, 1995.

545 R Development Core Team: R: a language and environment for statistical computing. R
546 Foundation for Statistical Computing, 2014.

547 Ravishankara, A. R., Daniel, J. S., and Portmann, R. W.: Nitrous oxide (N₂O): the dominant
548 ozone-depleting substance emitted in the 21st century, *Science*, 326, 123-125, 2009.

549 Röver, M., Heinemeyer, O., Munch, J. C., and Kaiser, E. A.: Spatial heterogeneity within the
550 plough layer: high variability of N₂O emission rates, *Soil Biol. Biochem.*, 31, 167-173,
551 1999.

552 Stein, A., van Dooremolen, W., Bouma, J., and Bregt, A. K.: Cokriging point data on
553 moisture deficit. *Soil Sci. Soc. Am. J.*, 52, 1418-1423, 1988.

554 Tokuda, S. I., and Hayatsu, M.: Nitrous oxide flux from a large amount of nitrogen fertilizer
555 and soil environmental factors controlling the flux, *Soil. Sci. Plant Nutr.*, 50, 365-374,
556 2004.

557 Turner, D. A., Chen, D., Gellbally, I. E., Li, Y., Edis, R. B., Leuning, R., Kelly, K., and
558 Phillips, F.: Spatial variability of nitrous oxide emissions from an Australian irrigated
559 dairy pasture, *Plant soil*, 309, 77-88, 2008.

560 Van den Pol-van Dasselaar, A., Corré, W. J., Klemedtsson, A., Weslien, P., Stein, A.,
561 Klemedtsson, L., and Oenema, O.: Spatial variability of methane, nitrous oxide, and
562 carbon dioxide emissions from drained grasslands, *Soil Sci. Soc. Am. J.*, 62, 810-817,
563 1998.

564 Van Kessel, C., Pennock, D.J., and Farrell, R.E.: Seasonal-variations in denitrification and
565 nitrous oxide evolution at the landscape scale, *Soil Sci. Soc. Am. J.*, 57, 988-995, 1993.

566 Velthof, G. L., Jarvis, S. C., Stein, A., Allen, A. G., and Oenema, O.: Spatial variability of
567 nitrous oxide fluxes in mown and grazed grasslands on a poorly drained clay soil, *Soil*
568 *Biol. Biochem.*, 28, 1215-1225, 1996.

569 Venterea, R. T., and Rolston, D. E.: Mechanisms and kinetics of nitric and nitrous oxide
570 production during nitrification in agricultural soil, *Glob. Change Biol.*, 6, 303-316, 2000.

571 Webster, R.: Quantitative spatial analysis of soil in the field, in: *Advances in Soil Science*,
572 edited by: Stewart, B.A., Springer, New York, 1-70, 1985.

573 Webster, R., and Oliver, M. A.: *Geostatistics for Environmental Scientists*, John Wiley &
574 Sons, Chichester, 2001.

575 Werner, C., Kiese, R., and Butterbach-Bahl, K.: Soil-atmosphere exchange of N₂O, CH₄, and
576 CO₂ and controlling environmental factors for tropical rain forest sites in western Kenya,
577 *J. Geophys Res.*, 112, D03308, doi:10.1029/2006JD007388, 2007.

578 Wrage, N., Velthof, G. L., Laanbroek, H. J., and Oenema, O.: Nitrous oxide production in
579 grassland soils: assessing the contribution of nitrifier denitrification, *Soil Biol. Biochem.*,
580 36, 229-236, 2004.

581 Yanai, J., Lee, C. K., Umeda, M., and Kosaki, T.: Spatial variability of soil chemical
582 properties in a paddy field. *Soil Sci. Plant Nutr.*, 46, 473-482, 2000.

583 Yanai, J., Sawamoto, T., Oe, T., Kusa, K., Yamakawa, K., Sakamoto, K., Naganawa, T.,
584 Inubushi, K., Hatano, R., and Kosaki, T.: Atmospheric pollutants and trace gases: spatial
585 variability of nitrous oxide emissions and their soil-related determining factors in an
586 agricultural field, *J. Environ. Qual.*, 32, 1965-1977, 2003.

587

588 Table 1 Descriptive statistics of the N₂O fluxes and environmental factors.

Variable ^a	Mean	Minimum	Maximum	CV (%)	Skewness of the original data	Skewness of the logit-transformed data
FLUX30	102.24 ^b	-1.73	1,659.11	234.7	4.37	0.6
ELEVATION	80.64	74.25	87.96	4.1	0.04	-
BD	1.26	0.90	1.56	10.1	-0.28	-
DOC	185.56	43.70	424.14	34.6	0.75	-
NH4N	62.33	1.89	842.55	190.8	3.28	0.17
NO3N	21.54	0.48	135.29	141.6	1.85	0.28
SOC	13.33	5.11	52.52	50.1	2.27	-0.44
TSN	1.52	0.81	4.12	38.3	1.73	-0.01
SWC	0.33	0.19	0.47	16.6	0.07	-
SAND	39.73	16.98	63.79	23.8	0.02	-
SILT	47.15	26.78	64.17	16.1	-0.29	-
CLAY	13.12	8.68	21.68	21.5	1.00	-

589 ^aFLUX30 is the N₂O flux (g N ha⁻¹ d⁻¹); ELEVATION is the elevation (m); and BD, DOC,
590 NH4N, NO3N, SOC, TSN, SWC, SAND, SILT and CLAY are the soil bulk density (Mg m⁻³),
591 soil dissolved organic carbon (mg C kg⁻¹ soil), soil ammonium (mg N kg⁻¹ soil), soil nitrate
592 (mg N kg⁻¹ soil), soil organic carbon (g C kg⁻¹ soil), soil total nitrogen (g N kg⁻¹ soil),

593 gravimetric soil water ($\text{g H}_2\text{O g}^{-1}$ soil), soil sand particle (%), soil silt particle (%) and soil
594 clay particle (%) content, respectively, of the 0-20 cm of topsoil.

595 ^bThe median and standard deviation of the FLUX30 were 27.56 and 239.96 $\text{g N ha}^{-1} \text{d}^{-1}$,
596 respectively.

597 Table 2 Semivariogram models for N₂O fluxes and the environmental factors.

Variable	Model	Nugget	Partial sill	Sill(nugget+ partial sill)	Distance Parameter (m)	Effective range (m)	Partial sill/sill
FLUX30t ^a	Exp	0	3.7186	3.7186	8.40	25.2	1.00
NH4Nt ^a	ND ^c	ND ^c	ND ^c	ND ^c	ND ^c	ND ^c	ND ^c
NO3Nt ^a	Ste	4.0794	0.6113	4.6907	91.92	163.7	0.13
SOct ^a	Sph	1.1198	0.7744	1.8942	92.96	93.0	0.41
TSNt ^a	Ste	1.0422	0.2816	1.3238	57.97	102.6	0.21
SWCt ^a	ND ^c	ND ^c	ND ^c	ND ^c	ND ^c	ND ^c	ND ^c
SAND ^a	ND ^c	ND ^c	ND ^c	ND ^c	ND ^c	ND ^c	ND ^c
SILT ^a	ND ^c	ND ^c	ND ^c	ND ^c	ND ^c	ND ^c	ND ^c
FLUX30t ^b	Exp	1.1911	2.0560	3.2471	17.36	52.1	0.63
NH4Nt ^b	Exp	2.0473	0.7185	2.7658	17.36	52.1	0.26
NO3Nt ^b	Exp	1.6241	1.1188	2.7429	17.36	52.1	0.41
SOct ^b	Exp	0.6043	1.0777	1.6820	17.36	52.1	0.64
TSNt ^b	Ste	0.9347	0.3114	1.2461	59.53	105.4	0.25
SWCt ^b	ND ^c	ND ^c	ND ^c	ND ^c	ND ^c	ND ^c	ND ^c
SAND ^b	ND	ND	ND	ND	ND	ND	ND
SILT ^b	ND	ND	ND	ND	ND	ND	ND

598 ND, not determined.

599 ^aSemivariogram models for the OK method.

600 ^bSemivariogram models for the RK method using the chamber placement position as the

601 auxiliary regression predictor.

602 ^cSpatial structures were not apparent.

603

604 Table 3 Statistics for N₂O fluxes during the dry and wet seasons.

Sample position	Mean	SD	Median	Max.	Min.	CV (%)
Dry season						
Inter-row (58)	5.15	4.95	4.09	22.43	-2.83	96.1
Fertilization point (50)	7.19	12.04	4.34	79.56	-6.42	167.4
Under tree (28)	3.58	2.91	2.36	10.28	0.68	81.3
In tree row (11)	5.95	10.38	3.98	52.17	-5.69	174.5
Wet season						
Inter-row (45)	101.69	287.23	27.56	1,659.11	-0.81	282.5
Fertilization point (45)	198.81	295.70	73.42	1,404.32	0.85	148.7
Under tree (22)	16.74	17.00	10.64	61.24	-1.73	101.6
In tree row (33)	28.30	38.34	14.72	177.08	0.19	135.5

605

606 The numbers in the parentheses represent the sample numbers for each chamber placement
 607 position.

608

609 Table 4 Cross-validations of the three different kriging interpolations for N₂O fluxes during
 610 the dry and wet seasons.

Method of spatial interpolation	Auxiliary variable	ME (no dimension)	RMSE (no dimension)	<i>r</i>	Predicted total N ₂ O emissions (g N d ⁻¹)
Dry season					
OK	-	0.0002	0.102	0.52	22.1 ^a
RK	ELEVATION	0.0008	0.098	0.57	21.1 ^a
CK	SOct	0.0006	0.103	0.51	22.0 ^a
CK	ELEV	0.0008	0.099	0.57	21.5 ^a
CK	SOct and ELEV	0.0009	0.098	0.57	21.2 ^a
Wet season					
OK	-	-0.0005	1.739	0.18	208.1
RK	POSITION	-0.0006	1.549	0.49	148.2
CK	SOct (POSITION)	0.0020	1.439	0.58	149.5
CK	NH4Nt (POSITION) and NO3Nt (POSITION)	0.0001	1.185	0.74	150.5

611 OK, RK and CK correspond to ordinary kriging, regression kriging and cokriging,
612 respectively; For the dry season campaign, ELEVATION, SOct and ELEV are the normalized
613 elevation, the normalized soil organic carbon content and the inverse of the normalized
614 elevation, respectively. For the wet season campaign, SOct, NH4Nt and NO3Nt are the
615 logit-transformations of soil organic carbon, soil ammonium and soil nitrate concentrations,
616 respectively. "POSITION" (in the parentheses) indicates the process of detrending the
617 influence of chamber placement position. The ME, RMSE, and r are the mean prediction
618 error, the root mean squared error (the mean squared deviation ratio of the prediction
619 residuals to the kriging standard errors), and the Pearson's correlation coefficient between the
620 observations and the predictions, respectively.

621 ^aThe predicted total N₂O emissions during the dry season were recalculated because the study
622 area changed from 4.8 ha to 4.0 ha for the wet season.

623

624 **Figure captions**

625

626 Figure 1. **(a, b)** Location and **(c, d)** digital elevation model and land use map of the tea
627 planted catchment. The red circles in **(c, d)** represent the sample points. The catchment is
628 located in Jinjing town, which is 70 km northeast of Changsha, the capital city of Hunan
629 Province, China.

630

631 Figure 2. Daily **(a)** air temperatures and **(b)** precipitation during 2012.

632

633 Figure 3. Histograms of **(a)** the original N₂O fluxes (FLUX30) and **(b)** the logit-transformed
634 N₂O fluxes (FLUX30t).

635

636 Figure 4. The Tukey's Honest Significant Difference analysis for FLUX30t, NH₄Nt, NO₃Nt,
637 SO₄t, TSNt and SWCt based on the four-chamber placement positions (R, inter-row; F,
638 fertilization point; U, under tea tree; and I, in the tea tree row).

639

640 Figure 5. Correlation matrix with the Pearson's correlation coefficients (r) of the N₂O fluxes
641 and the environmental factors. All of the variables in the correlation matrix are normally
642 distributed. FLUX30 represents the N₂O flux (g N ha⁻¹ d⁻¹); ELEVATION is the elevation (m);
643 and BD, DOC, NH₄N, NO₃N, SOC, TSN, SWC, SAND, SILT and CLAY are the soil bulk
644 density (Mg m⁻³), soil dissolved organic carbon (mg C kg⁻¹ soil), soil ammonium (mg N kg⁻¹

645 soil), soil nitrate (mg N kg^{-1} soil), soil organic carbon (g C kg^{-1} soil), total soil nitrogen (g N
646 kg^{-1} soil), gravimetric soil water ($\text{g H}_2\text{O g}^{-1}$ soil), soil sand particle (%), soil silt particle (%)
647 and soil clay particle (%) contents of the top 0-20 cm of the soil, respectively. Furthermore, *,
648 ** and *** represent the statistical significance at probability levels of 0.05, 0.01 and 0.001,
649 respectively. The lowercase letter t represents the logit transformation.

650

651 Figure 6. Semivariograms (open circles) and best-fitted models (solid lines) of the normal
652 logit-transformed N_2O fluxes (FLUX30t) (no dimension) for ordinary kriging (**a**) and the
653 regression residuals of FLUX30t (no dimension) with chamber placement position as the
654 predictor for regression kriging (**b**).

655

656 Figure 7. Direct and cross-semivariograms (open circles, detrending the influence of chamber
657 placement position for cokriging) and the best-fitted linear model of the co-regionalization
658 (solid lines) of the normal logit-transformed N_2O fluxes (FLUX30t) (no dimension) and the
659 normal SOC (SOCt, no dimension). The linear model of co-regionalization was characterized
660 by using the same range and different sills for its component models.

661

662 Figure 8. Direct and cross-semivariograms (open circles, detrending the influence of chamber
663 placement position for cokriging) and the best-fit linear model of co-regionalization (solid
664 lines) for the normal logit-transformed N_2O fluxes (FLUX30t) (no dimension), NH_4N
665 (NH_4Nt , no dimension) and NO_3N (NO_3Nt , no dimension). The linear model of

666 co-regionalization was characterized by the same range and different sills for its component
667 models.

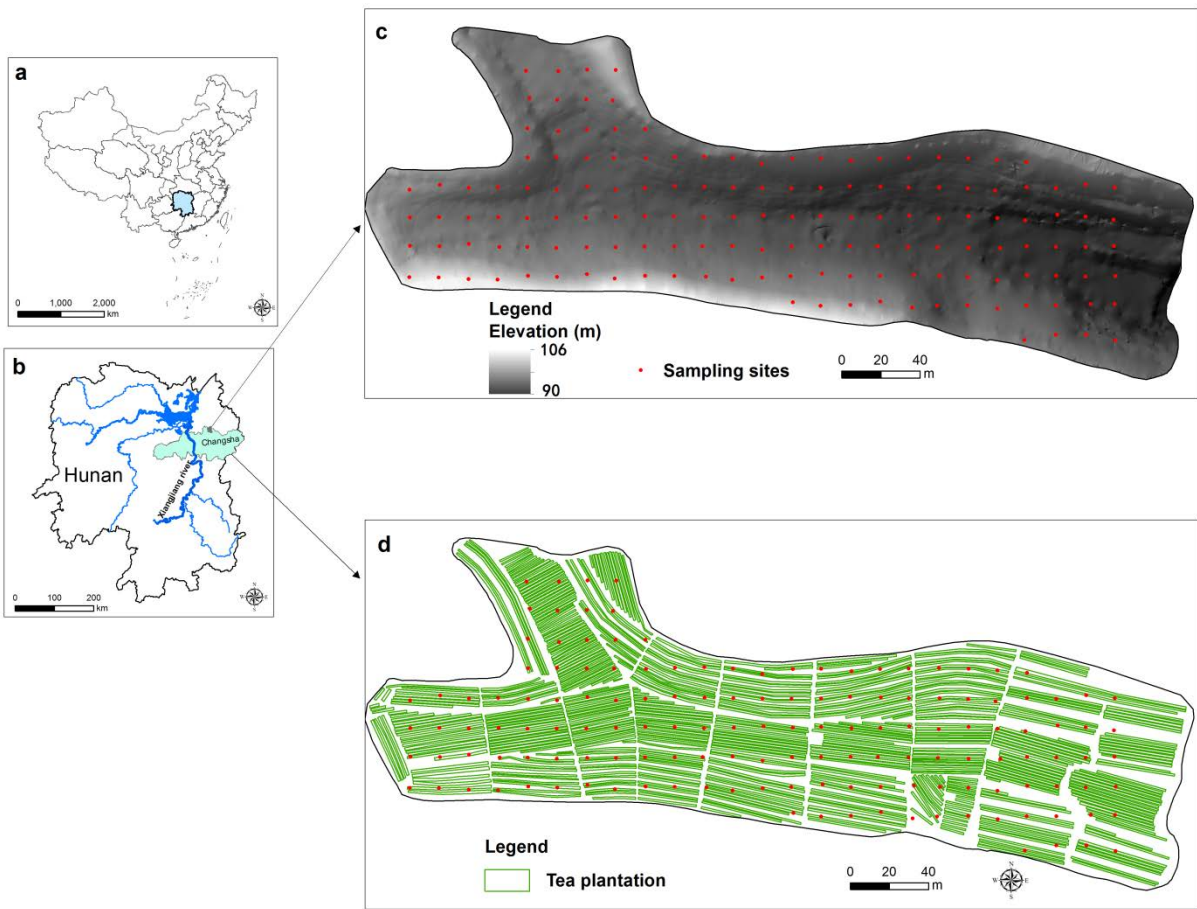
668

669 Figure 9. Spatial distributions of the N₂O fluxes as predicted by (a) OK, (b) RK with
670 chamber placement position as the regression predictor, (c) CK with SOCt (with the influence
671 of chamber placement position detrended) as the covariable, and (d) CK with NH₄Nt (with
672 the influence of chamber placement position detrended) and NO₃Nt (with the influence of
673 chamber placement position detrended) as two covariables. Here, SOCt, NH₄Nt and NO₃Nt
674 represent the logit-transformed soil organic carbon, soil ammonium and soil nitrate content,
675 respectively.

676

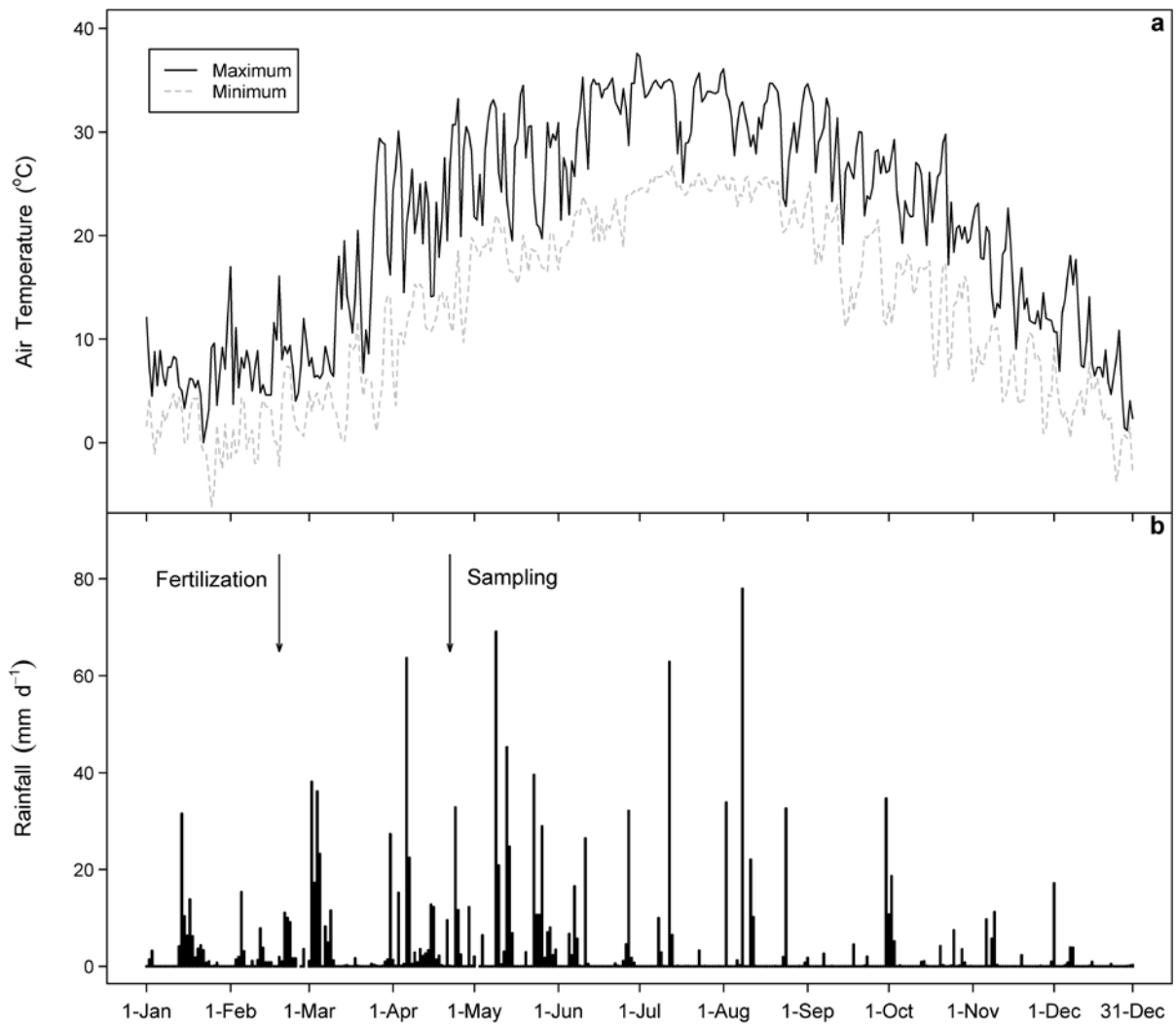
677 Figure 10. Spatial distributions of kriging standard deviations of the predicted N₂O fluxes by
678 (a) OK, (b) RK, (c) CK with SOCt as the covariable, and (d) CK with NH₄Nt and NO₃Nt as
679 two covariables.~~Figure 10. Spatial distributions of kriging variance of the N₂O fluxes as~~
680 ~~predicted by (a) OK, (b) RK with chamber placement position as the regression predictor, (c)~~
681 ~~CK with SOCt (with the influence of chamber placement position detrended) as the~~
682 ~~covariable, and (d) CK with NH₄Nt (with the influence of chamber placement position~~
683 ~~detrended) and NO₃Nt (with the influence of chamber placement position detrended) as two~~
684 ~~covariables. Here, SOCt, NH₄Nt and NO₃Nt represent the logit-transformed soil organic~~
685 ~~carbon, soil ammonium and soil nitrate content, respectively.~~

686



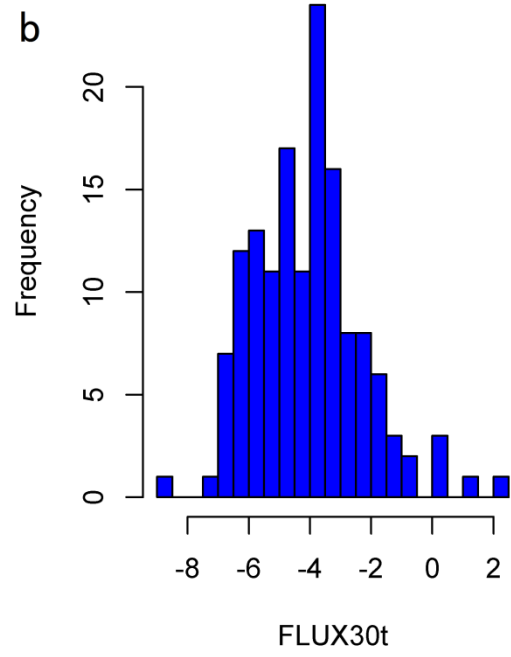
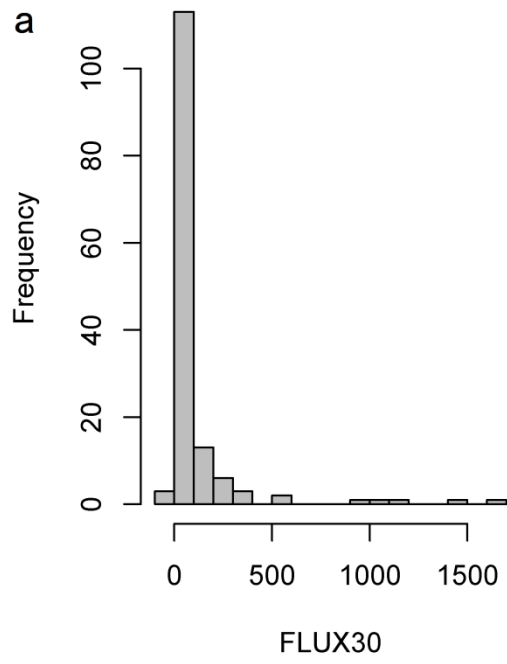
687

688 Figure 1



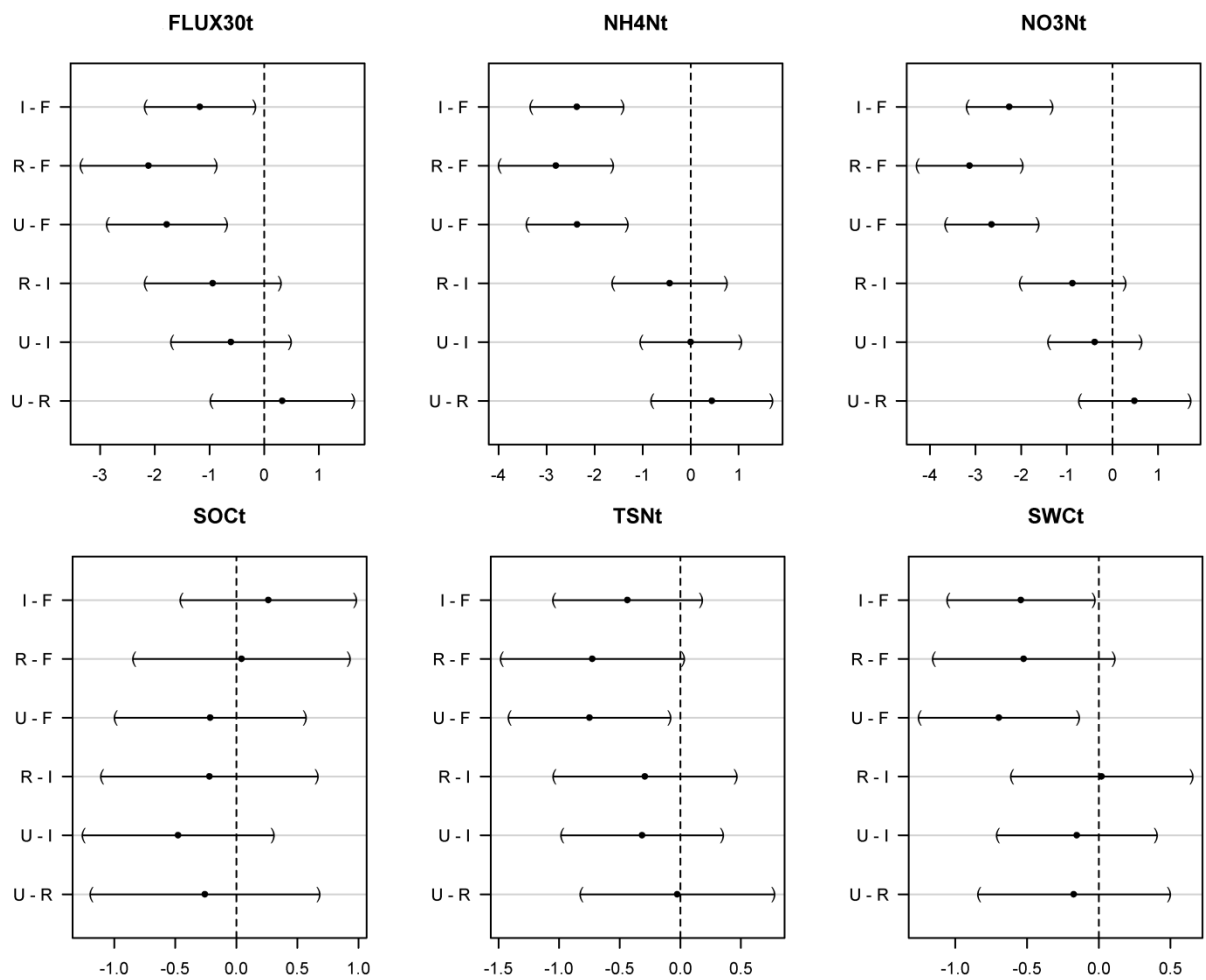
689

690 Figure 2



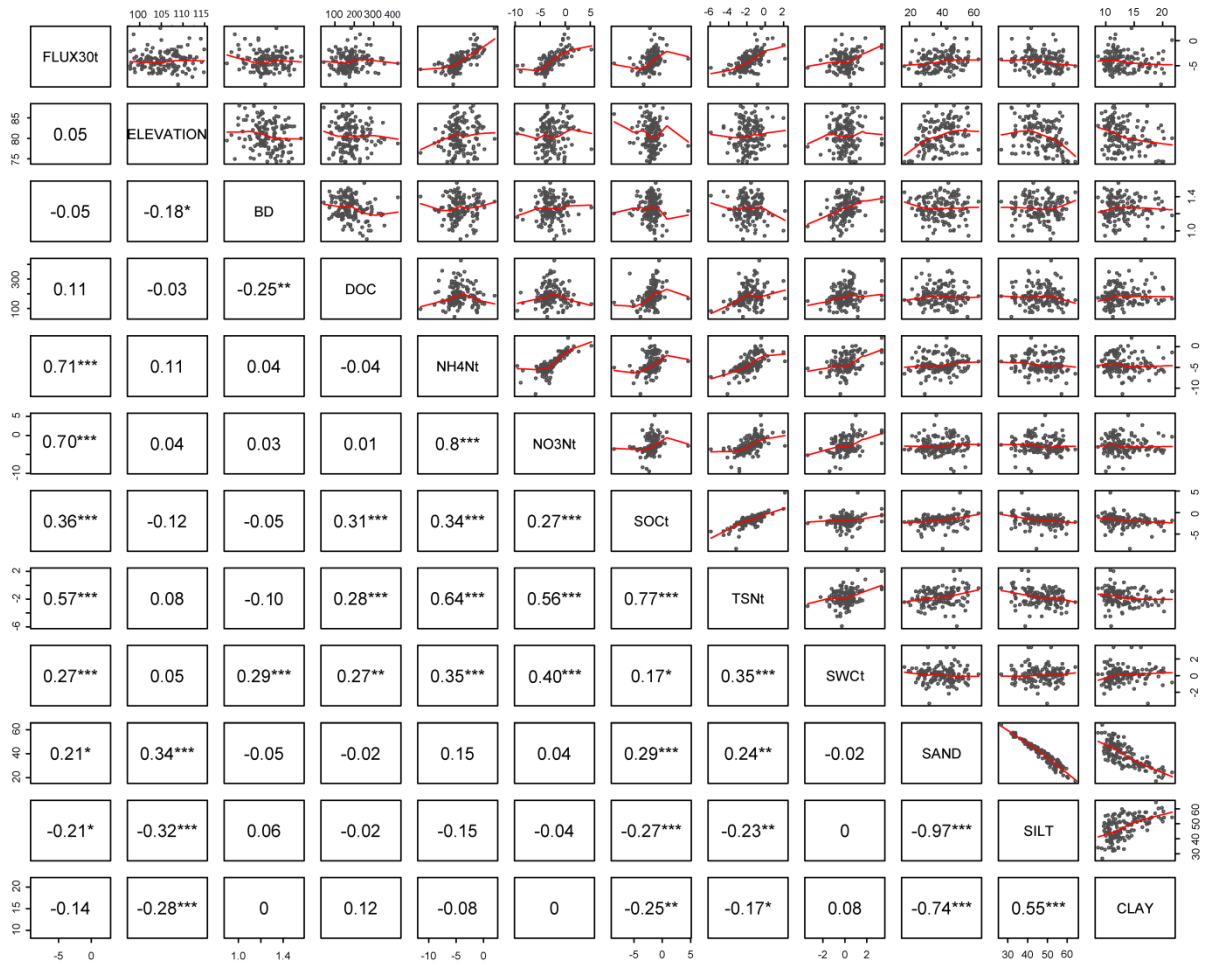
691

692 Figure 3



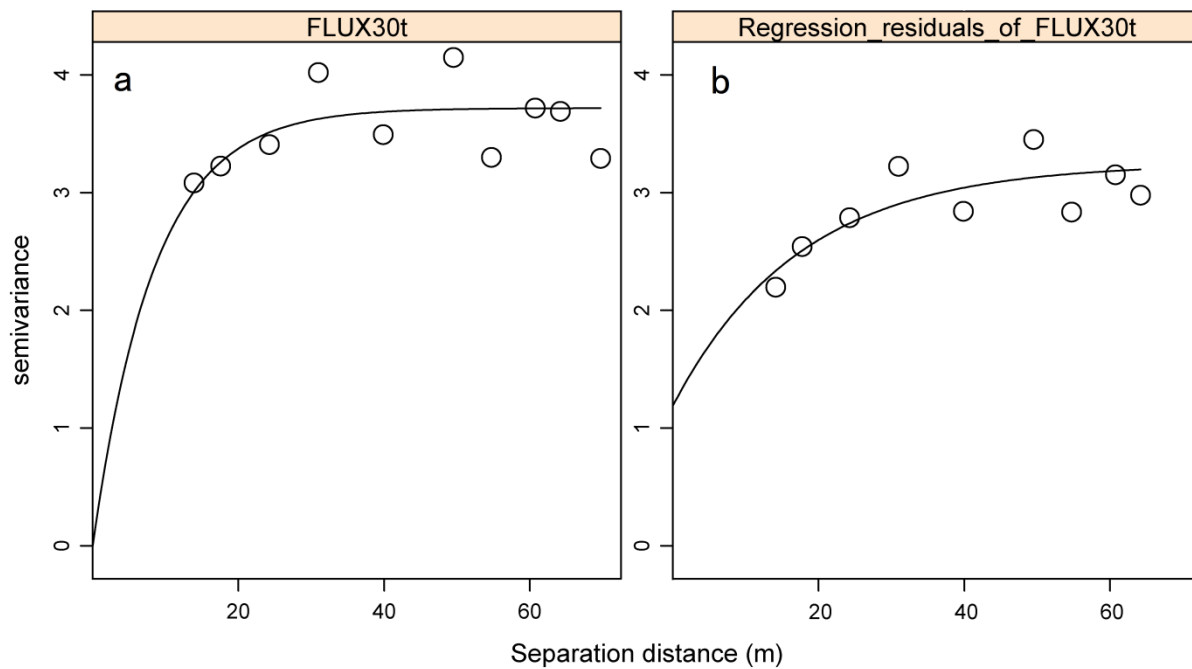
693

694 Figure 4



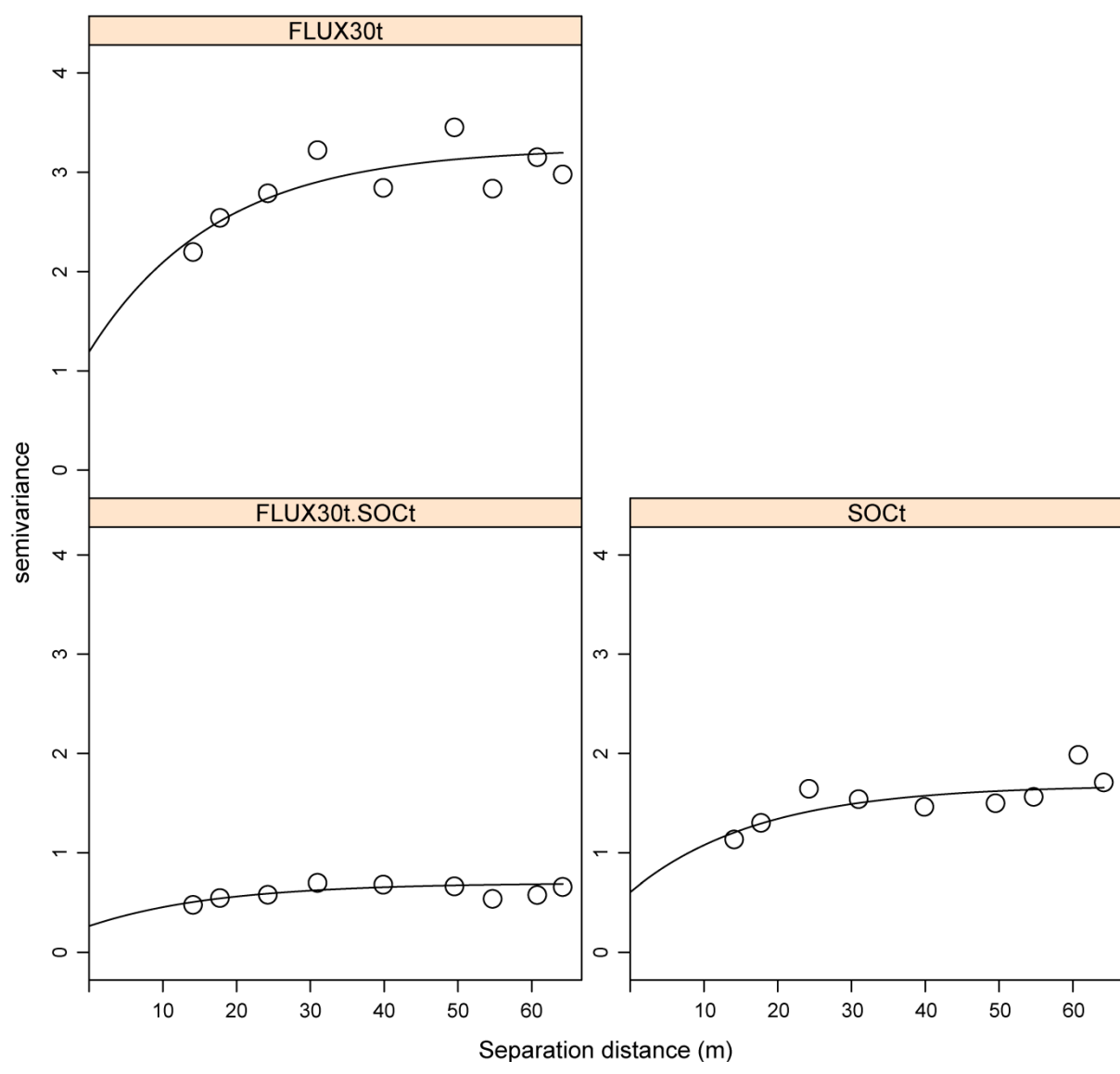
697 Figure 5

698



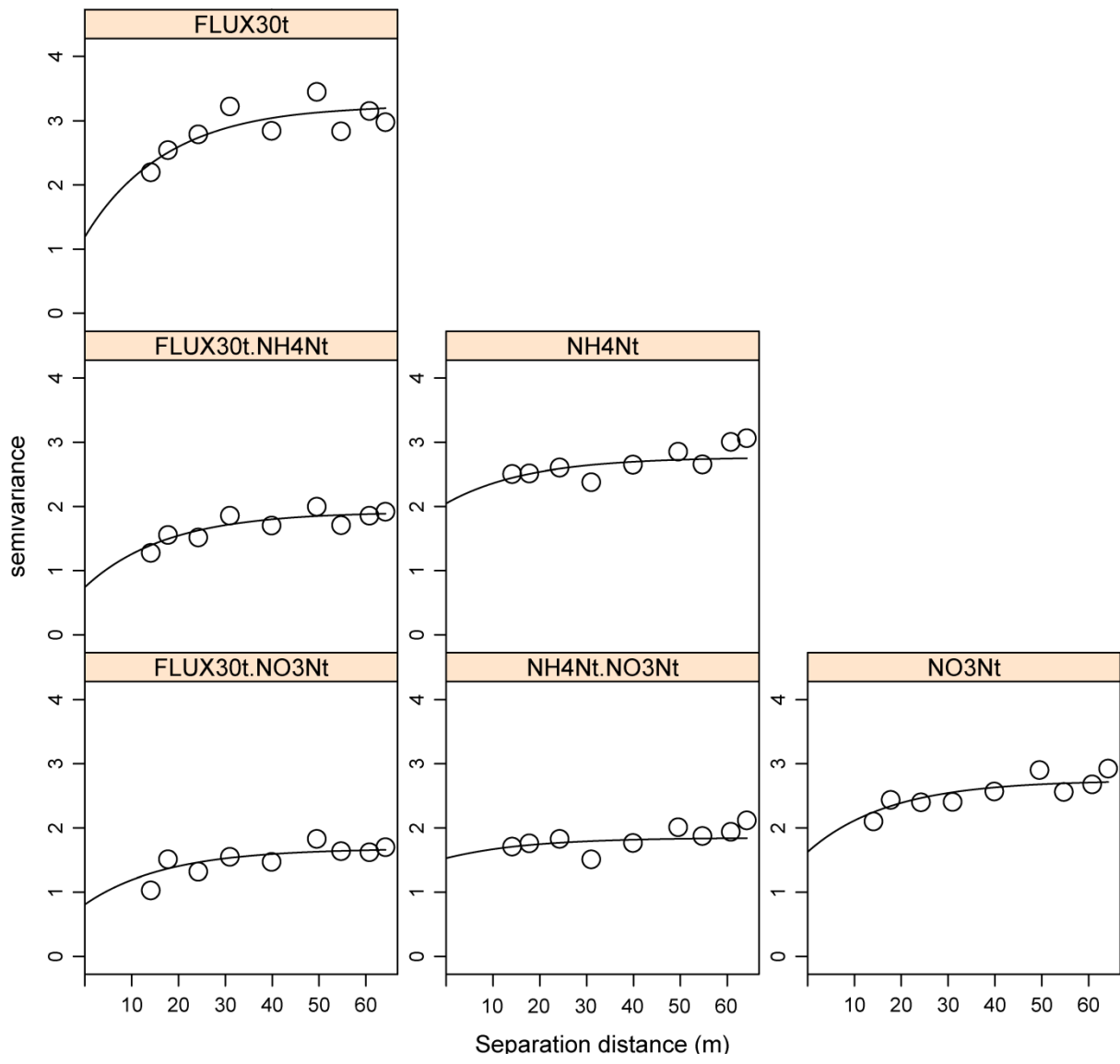
699

700 Figure 6



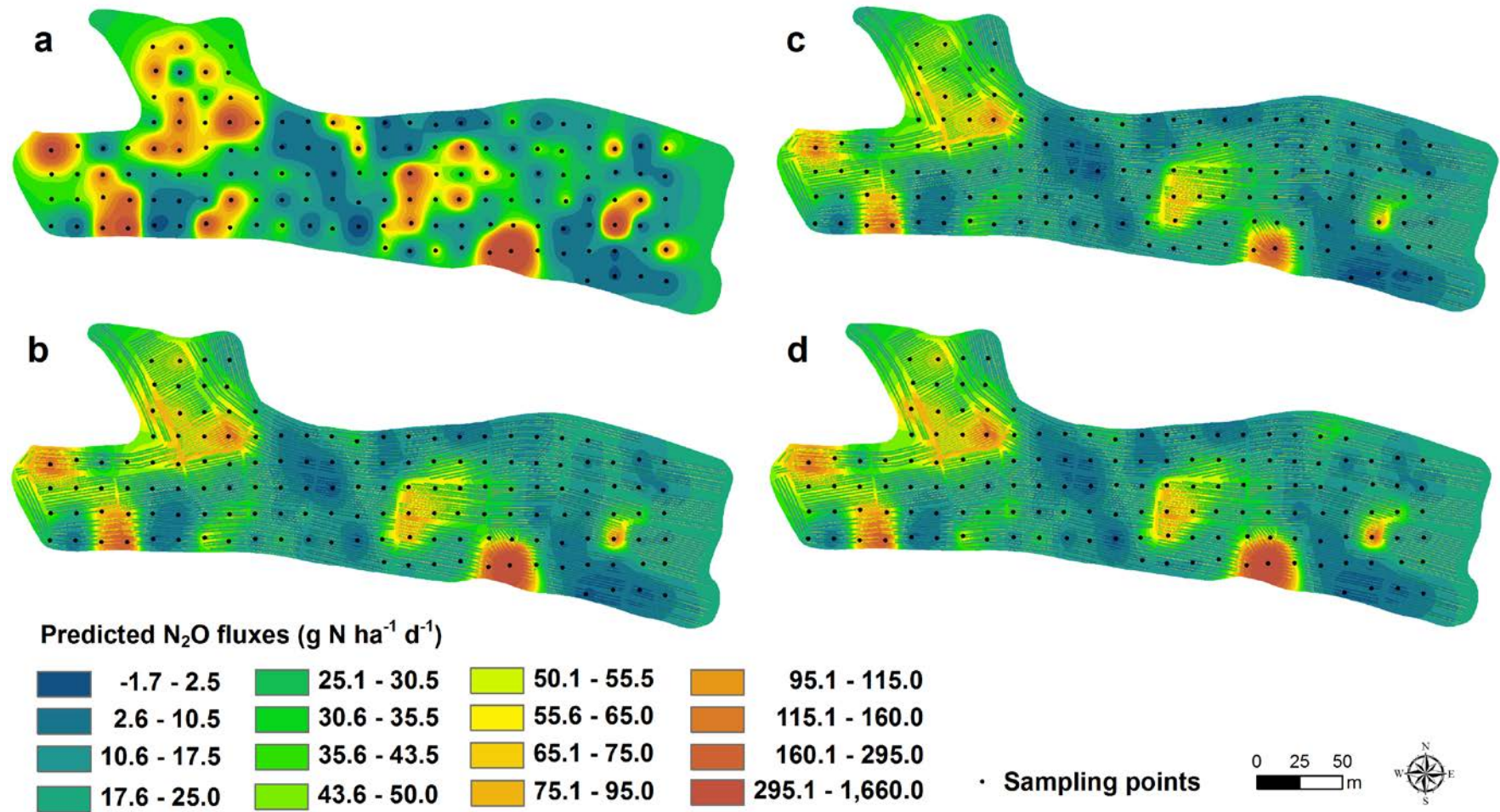
701
 702
 703
 704

Figure 7



705

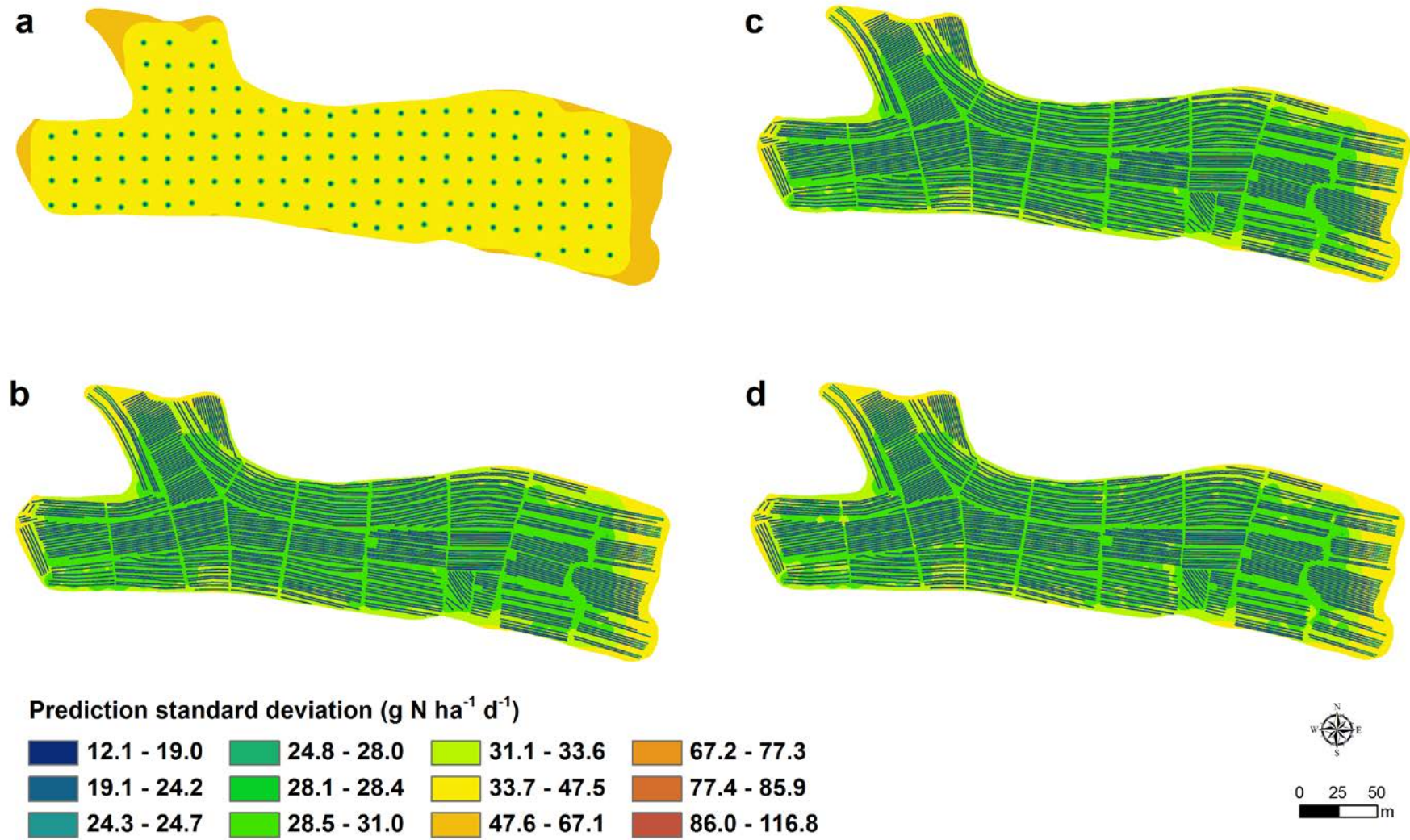
706 Figure 8



707

708 Figure 9

709



710

711 Figure 10